ESA Climate Change Initiative (CCI)

Climate Assessment Report (CAR)

for Climate Research Data Package No. 5 (CRDP#5)

of the Essential Climate Variable (ECV)

Greenhouse Gases (GHG)

Project: GHG-CCI+

Frédéric Chevallier [a]

[a] Laboratoire des Sciences du Climat et de l'Environnement (LSCE), Gif-sur-Yvette, France

Change log:

Version Nr.	Date	Status	Reason for change
Version 1.2	20 March 2020	Version finalised for CO_2, but without CH_4 further to Covid-19	

This document should be cited as:

Chevallier, F., Climate Assessment Report for the GHG-CCI+ project of ESA's Climate Change Initiative, pp. 36, version 1.2, 20 March 2020, 2020.

Table of content

1. Executive summary

This report describes the **assessment of the Essential Climate Variable (ECV) data products of the fifth release of the GHG-CCI Climate Research Data Package** (CRDP#5) by the Climate Research Group (CRG) of the GHG-CCI+ project (Buchwitz et al. 2015, 2017b; see also http://cci.esa.int/ghg). These products are CO_2 and CH_4 column retrievals (XCO_2 and XCH_4) from current satellite instruments:

- **CO2_OC2_FOCA:** XCO_2 from NASA's OCO-2 satellite retrieved by University of Bremen using the FOCAL algorithm (global, 2015-2018, v08)
- **CH4_S5P_WFMD:** XCH_4 from the European Sentinel-5-Precursor (S5P) satellite retrieved by University of Bremen using the WFM-DOAS algorithm (global, Nov. 2017 – Dec. 2018, v1.2)
- **CO2_TAN_OCFP:** XCO_2 from China's TanSat satellite retrieved by University of Leicester using the UoL-FP (or OCFP) algorithm (at TCCON sites, approx. 1 year, v1)

The global products CO2_OC2_FOCA and CH4_S5P_WFMD are (or will soon be) available (see status published at http://cci.esa.int/ghg) via the CCI Open Data Portal (http://cci.esa.int/data). In preparation are also the following products, which will be part of CRDP#6:

- XCO_2 and XCH_4 from Japan's GOSAT-2 satellite (products **CO2_GO2_SRFP**, **CH4_GO2_SRFP**, **CH4_GO2_SRPR**)

Climate researchers may find interest in these products for various reasons like evaluating climate models, estimating the uncertain parameters of these climate models, studying the variability of CO_2 and CH_4 in the atmosphere, studying wildfire or fossil fuel emission plumes, or quantifying the surface fluxes of these gases.

CRDP#5 is the first release of products from the GHG-CCI+ project, which started in March 2020.

Previous data sets, i.e., CRDP#1 – CRDP#4, have been generated and released by the GHG-CCI pre-cursor project (2010 - 2018). These products are CO_2 and CH_4 products from SCIAMACHY/ENVISAT, MIPAS/ENVISAT, GOSAT, AIRS and IASI. The XCO2 and XCH4 and IASI products are now generated operationally via the Copernicus Climate Change Service (C3S, https://climate.copernicus.eu/) and are available via the Copernicus Climate Data Store (CDS, https://cds.climate.copernicus.eu/).

By producing retrievals of the CO_2 and CH_4 columns for these satellites and others (ENVISAT and GOSAT in CRDP#1-4), CRDP has given a **unique**, though heterogeneous, **climate record from space covering now more than fifteen years** of the two major greenhouse gases of anthropogenic origin. **This length opens the possibility to characterize emission trends, as was already demonstrated by a series of CRDP-based studies for CH_4** (Bergamaschi et al. 2013) **and for CO_2** (Ross et al. 2013, Schneising et al. 2013a, 2013b, Reuter et al. 2014b, Detmers et al. 2015).

The pioneering character of these new climate records is deliberately acknowledged through the use of an ensemble of retrieval product covering several sensors and multiple retrieval algorithms (EMMA). **This ensemble approach allows a more comprehensive assessment of the product uncertainty than just the typical uncertainty characterisation of each product through internal uncertainty propagation**. Reuter et al. (2013, 2014a, 2020) well illustrated this capability.

The CRDP data sets, together with satellite retrievals made outside Europe, has already served to **quantify regional carbon budgets** (e.g., Basu et al. 2013, Bergamaschi et al. 2013, Fraser et al. 2013, Monteil et al. 2013, Cressot et al. 2013) and more specifically (for CO_2) Canada and Siberian forests (Schneising et al. 2011), Eurasia (Guerlet et al. 2013a), Tropical Asia (Basu et al. 2014), Amazonia (Parazoo et al. 2013) and Europe (Reuter et al. 2014a). However, for CO_2, there remain considerable discrepancies with bottom up estimates or flux inversions based on atmospheric in-situ observations (Chevallier et al. 2014a, 2019, Feng et al. 2016a, Reuter et al. 2016c). These discrepancies were also highlighted in the first four releases of the CAR (Chevallier et al. 2013, 2015, 2016, 2017). For CH_4 it has been clearly demonstrated that the SCIAMACHY retrievals and the GOSAT retrievals provide important information on regional methane emissions (e.g., Bergamaschi et al. 2013, Fraser et al. 2013, Alexe et al. 2015).

Each application of the CRDP has specific user requirements and it is not possible to exhaustively cover them in the CRG. Instead, the CRG has focussed on global source-sink inversion from several viewpoints.

<u>For CO_2</u>, the study has been restricted to the product in CRDP#5 that covers the whole globe and several years: CO2_OC2_FOCA which has been retrieved from OCO-2 over both land and ocean. The starting point of this report is the comparison between this product with the independent CAMS v18r3 transport model simulation (with surface fluxes inferred through inversion of high precision measurements of atmospheric CO_2 in situ samples). The satellite retrievals fit the independent CAMS simulation over land and ocean within 1.9 ppm RMS. By comparison and as expected, the ensemble product EMMA better fits the independent CAMS simulation, even when restricting the statistics to the 4 years of CO2_OC2_FOCA. However, further improved statistics are obtained when comparing NASA's ACOS OCO-2 retrievals, version 9, with the CAMS simulation over land as over ocean. This suggests that the individual ACOS retrievals have better precision than the CO2_OC2_FOCA ones.

The assimilation of the CO2_OC2_FOCA product in the LSCE global inversion system infers CO_2 surface fluxes that are very different from those obtained by the assimilation of surface air-sample measurements. The CO2_OC2_FOCA-driven CO_2 surface fluxes appear to be less credible because (i) the inferred spatial distribution of the ocean outgassing regions is inconsistent with current knowledge of the marine biogeochemistry obtained from sea surface CO_2 partial pressure measurements, (ii) the inferred atmospheric growth rate for year 2017 is notably different from the one seen at marine background stations, and (iii) the biases with aircraft data in the free troposphere are larger than when assimilation surface air-sample measurements. In contrast, the ACOS-driven CO_2 surface fluxes (ACOS being restricted to land retrievals here) seem to perform better than the CO2_OC2_FOCA-driven fluxes and even show comparable difference statistics to aircraft measurements in the free troposphere in output to the transport model compared to surface-air-sample-driven fluxes. This result demonstrates that there is no fundamental limitation to atmospheric inverse modelling (e.g., in the realism of the transport model or in the modelled error statistics) when assimilating satellite XCO_2 retrievals. It has also motivated the distribution of the ACOS-driven CO_2 surface fluxes as part of the official CAMS inversion products (this is version FT18r1 available from http://www.copernicus-atmosphere.eu/).

The various tests performed do not allow us to identify the distinctive asset of ACOS vs. CO2_OC2_FOCA in our system: either the data density, the data precision, the data trueness, the accuracy of the auxiliary data (averaging kernels) or a combination of these qualities at once. Detailed sensitivity tests could be performed for this. CO2_OC2_FOCA's distinct advantage compared to ACOS is its representation of multiple scattering effects in the radiative transfer in a form that is not costlier than absorption. In preparation for the Copernicus CO2 Monitoring Mission that will provide even larger amount of data than OCO-2, CO2_OC2_FOCA represents an important achievement. In this context and resources permitting, it would be important to document its performance with more detail in order to help prioritize future developments.

The section for CH_4 is in preparation but has been delayed because of Covid-19 related issues

2. User related aspects discussed in the peer-reviewed literature

The GHG-CCI project primarily aims at bringing new knowledge about the sources and sinks of CO_2 and CH_4 based on satellite-derived data products. Since the start of Phase 1 of the GHG-CCI pre-cursor project in 2010, this aspect has been addressed in a series of publications, which are shortly summarised in the following. They usefully provide the background for the new studies that have been performed specifically for this report and that will be described next. For a full list of publications see "Project publications" on http://cci.esa.int/ghg.

We start with the publications related to natural CO_2 fluxes.

- Using global GOSAT XCO_2 retrievals, Basu et al. (2013) presented first global CO_2 surface flux inverse modelling results for various regions. Their analysis suggested a reduced global land sink and a shift of the carbon uptake from the tropics to the extra-tropics. In particular, their results suggested that Europe is a stronger carbon sink than expected, but this feature was not further discussed in this paper.
- Chevallier et al. (2014a) analysed an ensemble of global inversion results assimilating two GOSAT XCO_2 retrieval products. They found hemispheric and regional differences in posterior flux estimates that are beyond 1 sigma uncertainties. They too found a significantly larger European carbon sink or a larger North African emission than expected. They concluded to the existence of significant flaws in all main components of the inversions: the transport model, the prior error statistics and the retrievals.
- Houweling et al. (2015) presented the outcome of a large inverse modelling intercomparison experiment on the use of GOSAT retrievals. The ensemble of results confirmed the large latitudinal shift in carbon uptake, but they showed that the reduced gradient degrades the agreement with background aircraft and surface measurements.
- Reuter et al. (2014a) investigated the European carbon sink further with another ensemble of GOSAT XCO_2 products, a SCIAMACHY XCO_2 product and a new inversion method which is less sensitive to some of the issues discussed in Chevallier et al. (2014a). Reuter et al. (2014a) only used satellite XCO_2 retrievals over Europe to rule out that non-European satellite data adversely influence the European results and they also only used short-term (days) transport modelling to avoid long-range transport errors. Based on an extensive analysis they concluded: "We show that the satellite-derived European terrestrial carbon sink is indeed much larger (1.02 ± 0.30 GtC/year in 2010) than previously expected". The value they derived is significantly larger compared to bottom-up estimates (not based on atmospheric measurements) of 0.235 ± 0.05 GtC/year for 2001-2004 (Schulze et al, 2009).
- The findings of Reuter et al. (2014a) stimulated additional research (Feng et al. 2016a, Reuter et al. 2016c).
- Detmers et al. (2015) analyzed GOSAT XCO_2 retrievals to detect and quantify anomalously large carbon uptake in Australia during a strong La Niña episode.
- For flux inversions not only the retrieved greenhouse gas values are relevant but also their error statistics, in particular the reported uncertainties. Chevallier and O'Dell (2013) analyzed this aspect in the context of CO_2 flux inversions using GOSAT XCO_2 retrievals. For CH_4, Cressot et al. (2013, 2016) studied the uncertainty of flux inversions assimilating SCIAMACHY, GOSAT or IASI XCH_4 retrievals.
- Focussing on Canadian and Siberian boreal forests, Schneising et al. (2011) computed longitudinal XCO_2 gradients from SCIAMACHY XCO_2 retrievals during the vegetation growing season over Canadian and Siberian boreal forests and compared the gradients with outputs from NOAA's CO_2 assimilation system CarbonTracker (Peters et al. 2007). They found good agreement for the total

boreal region and for inter-annual variations. For the individual regions, however, they found systematic differences suggesting a stronger Canadian boreal forest growing season CO_2 uptake and a weaker Siberian forest uptake compared to CarbonTracker.

- Focussing on hemispheric data and on carbon-climate feedbacks, Schneising et al. (2014a) used SCIAMACHY XCO_2 to study aspects related to the terrestrial carbon sink by looking at co-variations of XCO_2 growth rates and seasonal cycle amplitudes with near-surface temperature. They found XCO_2 growth rate changes of 1.25 ± 0.32 ppm/year/K (approximately 2.7 ± 0.7 GtC/year/K; indicating less carbon uptake in warmer years, i.e., a positive carbon-climate feedback) for the Northern Hemisphere in good agreement with CarbonTracker.
- Reuter et al. (2013) computed CO_2 seasonal cycle amplitudes using various satellite XCO_2 data products (using GHG-CCI products but also GOSAT XCO_2 products generated in Japan at NIES (Yoshida et al. 2013, Oshchepkov et al. 2013) and the NASA ACOS product (O'Dell et al. 2012) and compared the amplitudes with TCCON and CarbonTracker. They found that the satellite products typically agree well with TCCON but they found significantly lower amplitudes for CarbonTracker suggesting that CarbonTracker underestimates the CO_2 seasonal cycle amplitude by approx. 1.5 ± 0.5 ppm (see also Buchwitz et al., 2015, for a discussion of these findings).
- Lindquist et al. (2015) compared satellite XCO_2 retrievals, surface XCO_2 retrievals and atmospheric model simulations in terms of XCO_2 seasonal cycle. They found that the satellite retrieval algorithms performed qualitatively similarly but showed notable scatter at most validation sites. None of the tested algorithm clearly outperformed another. They showed that the XCO_2 seasonal cycle depends on longitude especially at the mid-latitudes, which was only partially shown by the models. They also found that model-to-model differences could be larger than GOSAT-to-model differences.
- Guerlet et al. (2013a) analyzed GOSAT XCO_2 retrievals focusing on the Northern Hemisphere. They identified a reduced carbon uptake in the summer of 2010 and found that this is most likely due to the heat wave in Eurasia driving biospheric fluxes and fire emissions. Using a joint inversion of GOSAT and surface data, they estimated an integrated biospheric and fire emission anomaly in April–September of 0.89 ± 0.20 PgC over Eurasia. They found that inversions of surface measurements alone fail to replicate the observed XCO_2 inter-annual variability (IAV) and underestimate emission IAV over Eurasia. They highlighted the value of GOSAT XCO_2 in constraining the response of land-atmosphere exchange of CO_2 to climate events.
- Basu et al. (2014) studied seasonal variation of CO_2 fluxes during 2009-2011 over Tropical Asia using GOSAT, CONTRAIL and IASI data. They found an enhanced source for 2010 and concluded that this is likely due to biosphere response to above-average temperatures in 2010 and unlikely due to biomass burning emissions.
- Parazoo et al. (2013) used GOSAT XCO_2 and solar induced chlorophyll fluorescence (SIF) retrievals to better understand the carbon balance of southern Amazonia.
- Ross et al. (2013) used GOSAT data to obtain information on wildfire CH_4:CO_2 emission ratios.

Despite the fact that none of the existing satellite missions has been optimized to obtain information on anthropogenic CO_2 emissions, this important aspect has been addressed in several recent publications using existing satellite XCO_2 products.

- Schneising et al. (2013) presented an assessment of the satellite data over major anthropogenic CO_2 source regions. They used a multi-year SCIAMACHY XCO_2 data set and compared the regional XCO_2 enhancements and trends with the emission inventory EDGAR v4.2 (Olivier et al. 2012). They found no significant trend for the Rhine-Ruhr area in central Europe and the US East Coast but a significant increasing trend for the Yangtze River Delta in China of about 13 ± 8%/year, in agreement with EDGAR (10 ± 1%/year).

- Reuter et al. (2014b) studied co-located SCIAMACHY XCO_2 and NO_2 retrievals over major anthropogenic source regions. For East Asia they found increasing emissions of NO_x (+5.8%/year) and CO_2 (+9.8%/year), i.e., decreasing emissions of NO_x relative to CO_2 indicating that the recently installed and renewed technology in East Asia, such as power plants and transportation, is cleaner in terms of NO_x emissions than the old infrastructure, and roughly matches relative emission levels in North America and Europe.

A series of studies also addressed methane emissions.

- SCIAMACHY data have already been extensively used to improve our knowledge on regional methane emissions prior to the start of the GHG-CCI project (e.g., Bergamaschi et al. 2009). A more recent research focus was to shed light on the unexpected renewed atmospheric methane increase during 2007 and later years using ground-based and satellite data (e.g., Rigby et al. 2008, Dlugokencky et al. 2009, Bergamaschi et al. 2009, 2013, Schneising et al. 2011, Frankenberg et al. 2011, Sussmann et al. 2012, Crevoisier et al. 2013). Based on an analysis of SCIAMACHY year 2003-2009 retrievals an increase of 7-9 ppb/year (0.4-0.5%/year) has been found with the largest increases in the tropics and northern mid latitudes (Schneising et al. 2011) but a particular region responsible for the increase has not been identified (Schneising et al. 2011; Frankenberg et al. 2011). Bergamaschi et al. (2013) used SCIAMACHY retrievals and NOAA surface data for 2003-2010 and inverse modelling in order to attribute the observed increase of atmospheric concentrations to changes in emissions. They concluded that most of this increase is due to emissions in the Tropics and the mid-latitudes of the northern hemisphere, while no significant trend was derived for Arctic latitudes. The increase is mainly attributed to anthropogenic sources, superimposed with significant inter-annual variations of emissions from wetlands and biomass burning.
- Methane emissions have also been obtained from GOSAT, as presented in a number of publications as shown in, e.g., Fraser et al. (2013, 2014), Monteil et al. (2013), Cressot et al. (2014), Alexe et al. (2015), Turner et al. (2015) and Pandey et al. (2016). Note that for these studies often CH_4 retrievals from several satellites have been used (as well as NOAA data), e.g., Monteil et al. (2013), and Alexe et al. (2015) used SCIAMACHY and GOSAT retrievals and Cressot el al. (2014, 2016) used GOSAT, SCIAMACHY and IASI. Alexe et al. (2015) showed that the different satellite products resulted in relatively consistent spatial flux adjustment patterns, particularly across equatorial Africa and North America. Over North America, the satellite inversions result in a significant redistribution of emissions from North-East to South-Central USA, most likely due to natural gas production facilities.
- Several publications focused on (relatively localized) methane sources in the United States: For example, Schneising et al. (2014b) analyzed SCIAMACHY data over major US "fracking" areas and quantified methane emissions and leakage rates. For two of the fastest growing production regions in the US, the Bakken and Eagle Ford formations, they estimated that emissions increased by 990 ± 650 $ktCH_4$/year and 530 ± 330 $ktCH_4$/year between the periods 2006–2008 and 2009–2011. Relative to the respective increases in oil and gas production, these emission estimates correspond to leakages of 10.1% ± 7.3% and 9.1% ± 6.2% in terms of energy content, calling immediate climate benefit into question and indicating that current inventories likely underestimate the fugitive emissions from Bakken and Eagle Ford. Others also used SCIAMACHY data over the US to identify and quantify localized anthropogenic methane emission sources (Kort et al. 2014, Wecht et al. 2014). Last, Turner et al. (2015) used GOSAT retrievals within a meso-scale inversion system for the US.

The SCIAMACHY XCH_4 retrievals have also been used to improve chemistry-climate models (Shindell et al. 2013, Hayman et al. 2014).

3. Assessment of satellite-derived XCO_2 products

3.1. Introduction

Given nearly a decade (since Basu et al., 2013, see Section 2) of global inverse modelling studies assimilating real XCO_2 retrievals, extended to 1.5 decades (Chevallier et al., 2005) in the case of partial column CO_2 retrievals, the current interest in XCO_2 products for global inverse modelling is about multi-year global products. This has not been always the case (Chevallier et al, 2011). The first four GHG-CCI Climate Research Data Packages fulfilled this ambition with SCIAMACHY and TANSO retrievals.

The 5th GHG-CCI+ Climate Research Data Package (CRDP#5, http://cci.esa.int/ghg#data) includes three products:

- CO2_OC2_FOCA: retrieved from OCO-2 using University of Bremen's FOCAL algorithm
- CO2_TAN_OCFP: retrieved from TanSat using University of Leicester's UoL-FP (or OCFP) algorithm
- CO2_GO2_SRFP: retrieved from GOSAT-2 using SRON's RemoTeC (or SRFP) algorithm

At the scale of the GHG-CCI+ project, the goal for all three is to make multi-year global products available, but currently only the first one, CO2_OC2_FOCA, fulfils this criterion. It is evaluated in this section. We have also looked at the latest version of the ensemble median algorithm EMMA for a shorter evaluation. EMMA was initially co-developed by GHG-CCI and is now distributed by C3S (https://cds.climate.copernicus.eu/cdsapp#!/dataset/satellite-carbon-dioxide).

The two evaluated products are summarized in Table 1 below. The official bias-corrected products have been processed by LSCE.

Product ID	Instrument	Algorithm	Data provider	Reference	Period available	Evaluators (sections)
CO2_OC2_FOCA	OCO-2	FOCAL, v8	IUP, Univ. Bremen	Reuter et al., 2017a, 2017b	01/2015-12/2018	LSCE (3.2, 3.3)
XCO2_EMMA	SCIAMACHY + TANSO + OCO-2	EMMA, v4.1	IUP, Univ. Bremen	Reuter et al., 2020	01/2003-12/2018	LSCE (3.2)

Table 1. XCO_2 products evaluated in this report.

3.2. Comparisons with model simulations

3.2.1. Method

In this section, we compare CO2_OC2_FOCA and XCO2_EMMA with a forward simulation of the LMDZ transport model (Hourdin et al. 2006) nudged to the ERA5 reanalysis and using surface fluxes from a classical atmospheric inversion that assimilated surface air-sample measurements. The simulation accounts for the prior profiles and the averaging kernels of each individual retrieval. Chevallier and O'Dell (2013) showed that the uncertainty of such simulated XCO_2 field is small (standard deviation is less than 0.85 ppm) compared to XCO_2 retrieval errors from GOSAT, even over Tropical lands, so that the model-minus-retrieval departures are dominated by the retrieval errors. The accuracy of the surface air-sample-driven inversion is also confirmed by comparison to TCCON retrievals (Chevallier, 2019). Computing the departures therefore allows evaluating the realism of the product retrieval errors that are an integral part of the L2 retrieval process. We refer to Chevallier and O'Dell (2013) for more background about the underlying principles. We add a third XCO_2 retrieval product in the comparison: version 9 of the Atmospheric CO_2 Observations from Space (ACOS) retrievals of O'Dell et al. (2018) from OCO-2. We use it because it is currently the main OCO-2 retrieval product in use in the science community.

The CO2_OC2_FOCA and XCO2_EMMA date files do not make the distinction between land and ocean retrievals and we do not attempt at getting this information from some other source using the latitude and longitude coordinates. Since the fraction of land in the sounding is reported in the ACOS product, we stratify the results per geotype: land is defined by a land fraction larger than 80%.

Our forward simulation comes from the CAMS CO_2 inversion product driven by surface air-sample measurements (version 18r3, http://www.copernicus-atmosphere.eu/), an earlier version of which was described by Chevallier et al. (2010a). It uses the LMDZ transport model with a recent configuration of the model physics (Remaud et al., 2018). In space, the model is discretized into 39 vertical layers, 3.75 longitude degrees and 1.9 latitude degrees.

The OCO-2 retrievals have much higher spatial resolution than the global LMDZ model, by several orders of magnitude. The locations of successive footprints are also close to each other. To account for this locally-high density, we follow Crowell et al. (2019) by aggregating the OCO-2 retrievals from CO2_OC2_FOCA and ACOS in 10-second intervals, that roughly correspond to boxes of 67×10 km^2, a surface area which is still much smaller than the individual model grid boxes of 3.75° × 1.9 °. XCO2_EMMA applies a different strategy in which large datasets like the OCO-2 are thinned randomly rather than aggregated at coarser resolution (Reuter et al., 2020). We therefore do not apply the 10-second binning algorithm to it.

3.2.2. Results

Multiyear-results are summarized in Figure 1. Distinction is made between the latitudes north of 25°N, the latitudes south of 25°S and the latitudes between 25°S and 25°N. Since we have no way to distinguish between random errors and systematic ones in the retrieval products and in the forward simulation, and following the usual practice (e.g., Desroziers et al. 2005), we use the root mean square (RMS) to characterize the statistics of the model-minus-observation departures, rather than the standard deviation.

The number of data feeding the statistics (the pink bars in Figure 1) varies with the product type (much more data in the hybrid 16-year-long XCO2_EMMA than in the two OCO-2 products) and with the screening performed in the corresponding retrieval algorithm (much more data in ACOS than in CO2_OC2_FOCA). The RMS departures (the orange disks in Figure 1) are between 1.2 and 1.9 ppm for CO2_OC2_FOCA. They are better for XCO2_EMMA North of 25°N and similar in the two other bands. The better statistics North of 25°N also hold when restricting them to the CO2_OC2_FOCA period. This is explained by the better statistics of ACOS, even over land only (bottom left plot), and, likely, by the selection algorithm of XCO2_EMMA that damps retrieval noise.

The precision and bias of CO2_OC2_FOCA has been assessed independently (Table 5 in Product Validation and Intercomparison Report, PVIR, Buchwitz et al. 2020) based on TCCON observations (Wunch et al. 2011). The scatter of the retrieval misfits to TCCON is overall similar to the scatter of the retrieval misfits to the model.

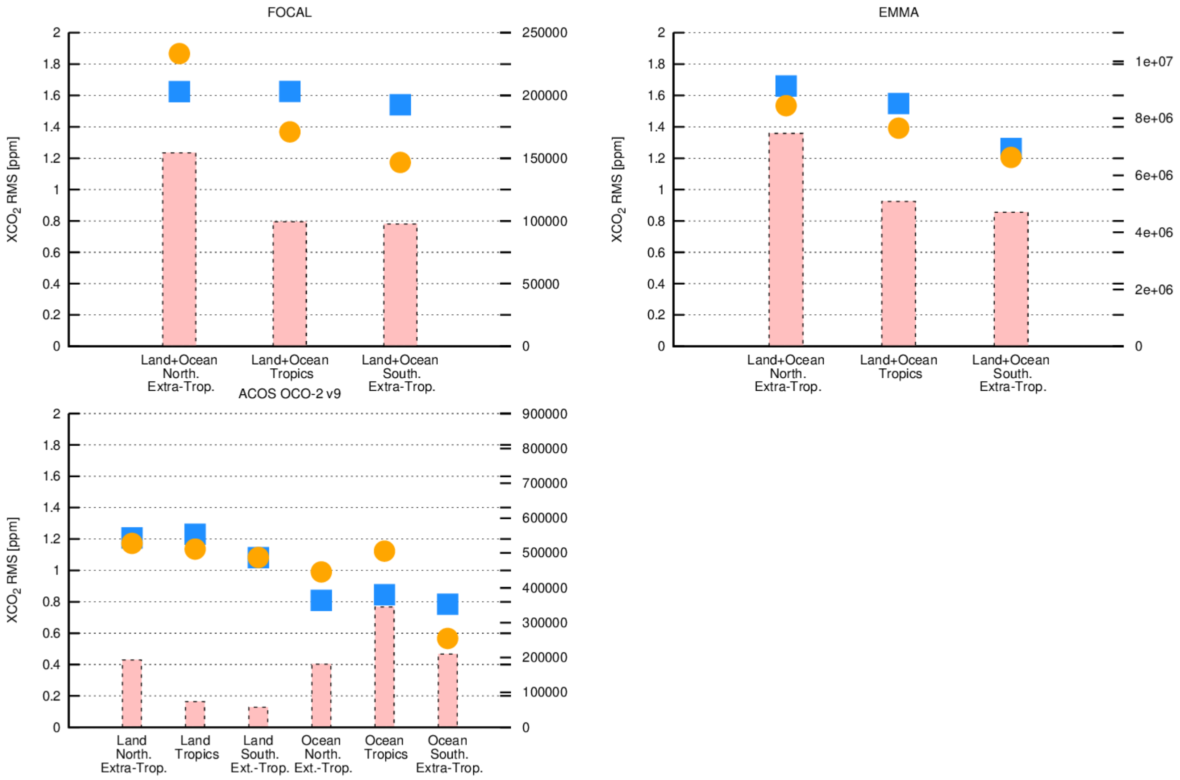

Figure 1. The orange disks show the Root Mean Squared values (RMS) of the misfits between the three XCO_2 products indicated in the plot titles and the reference CAMS surface-driven simulation for the full period covered by each retrieval product. The blue squares represent the root mean square of the sum of the CAMS simulation error variances and of the retrieval error variances. The globe is divided into three latitude bands. For ACOS only, as in the corresponding data files, land and ocean are separated. The number of data included in the statistics is reported as vertical pink bars.

We now look at the retrieval error statistics provided by each product (the blue squares in Figure 1). In the study by Chevallier and O'Dell (2013), the model-data misfits with GOSAT retrievals showed good consistency with the documented retrieval errors, to the point that the theoretical error reduction brought by the surface measurements on the simulation of the GOSAT total column measurements (15%) corresponded to the actual reduction seen over the mid-latitude and Tropical lands and over the Tropical oceans. The retrieval uncertainty reported in the data files of XCO2_EMMA appears to be fairly estimated, but the one in CO2_OC2_FOCA shows more difference with the actual departure statistics. In the case of ACOS, a good fit of the statistics is seen over land, less so over the ocean.

3.3. Inversion experiments with the LSCE system

3.3.1. Method

In this section, we go one step further in the evaluation of CO2_OC2_FOCA with the LSCE system by interpreting the model-data misfits shown in Section 3.2 in terms of surface fluxes. We do not do the same for XCO2_EMMA by lack of resources to process this 16-year-long product within a reasonable timescale for the project. The satellite data are assimilated alone, without combining them with other observations, in order to focus on their own signals. We use CO2_OC2_FOCA candidly, i.e. without modifying the retrieval values and their associated uncertainty in input to the 10-s binning algorithm described in Section 3.2.1. However, if several 10-s-binned retrievals of a same orbit fall within the same model grid box, we inflate the variance of the retrieval errors by the number of concerned 10-s-binned retrievals, in order to avoid likely local error correlations (at least from the transport model). As in the previous section, we use the retrieval averaging kernels and prior profiles when assimilating them. Processing the full multi-year series of CO2_OC2_FOCA within the inverse system required about one month of computation on 10 parallel CPU cores.

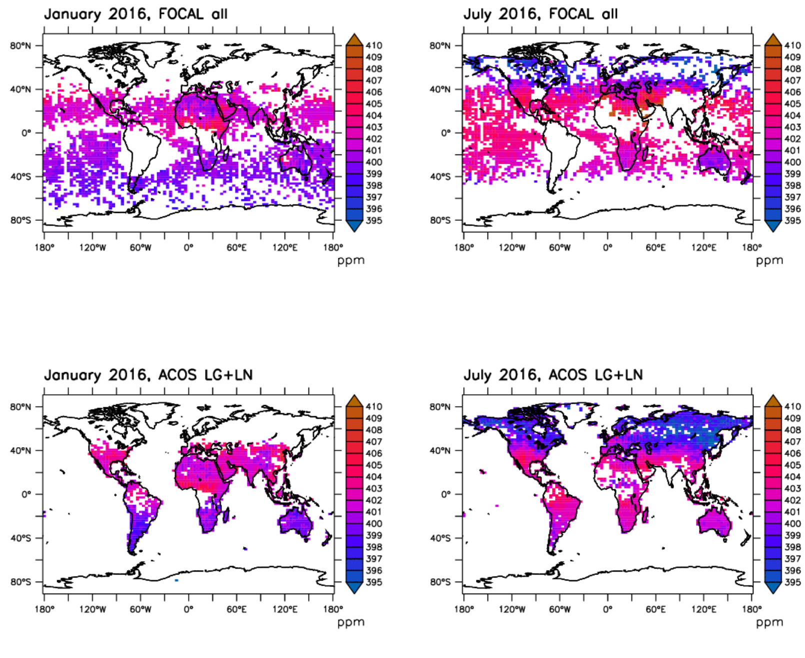

Figure 2. Average of the retrievals (as they are assimilated here) in each model grid box for January and July 2016. CO2_OC2_FOCA (both lands and oceans) and ACOS (land only) are shown in the top and bottom rows, respectively.

The fluxes inferred from CO2_OC2_FOCA are compared to two benchmark inversion: the CAMS official inversion products v18r3 that exclusively assimilated about 130 sites of surface air-sample measurements from the Global Atmosphere Watch programme and the CAMS official inversion product FT18r1 that exclusively assimilated the ACOS OCO-2 retrievals over land. Ocean glint retrievals were not assimilated in FT81r1 because of likely systematic errors (Chevallier et al., 2019), but such a selection is not done for CO2_OC2_FOCA here in the absence of similar evidence. Still, many more ACOS retrievals are assimilated than CO2_OC2_FOCA ones in the respective inversions (see Figure 1) due to much stricter filter criteria that leave large regions unobserved or poorly observed during full months in the latter (Figure 2).

The inversion system works at the grid-point weekly scale and generates a large volume of data. The present comparison focuses on a few key quantities: (i) the global annual growth rate that is well known from the NOAA marine surface data (Conway et al. 1994, http://www.esrl.noaa.gov/gmd/ccgg/trends/global.html), (ii) the grid-point annual-total fluxes, (iii) the regional annual CO_2 budgets.

3.3.2. Global annual atmospheric growth rates

Figure 3 shows the time series of the global annual growth rates from NOAA, from the CAMS inversions and from CO2_OC2_FOCA. We use a conversion factor of 2.086 $GtC \cdot ppm^{-1}$ from Prather (2012). Note that the NOAA estimate and the surface-driven CAMS one are not independent since the surface-driven CAMS inversion assimilates the individual NOAA measurements. Their difference has a standard deviation of 0.16 ppm and a bias of -0.02 ppm (based on 40 yearly values). The statistics estimate for the OCO-2-driven CAMS inversion is of 0.00±0.12 ppm (the estimate is based on 4 annual values). The difference between the growth rate from the CO2_OC2_FOCA inversion and the NOAA estimate is larger: a bias of -0.13 ppm and a standard deviation of 0.22 ppm (based on 4 values). This is driven by year 2017 for which the CO2_OC2_FOCA inversion diagnoses a much smaller growth rate than NOAA. Note that the quality of the growth rate of the CO2_OC2_FOCA retrievals themselves may be much better, but since they do not cover the full globe all the time, the inversion system, informed by the transport model (hard constraint), may generate very different XCO_2 between the retrievals, for instance to fit small spurious retrieval signals.

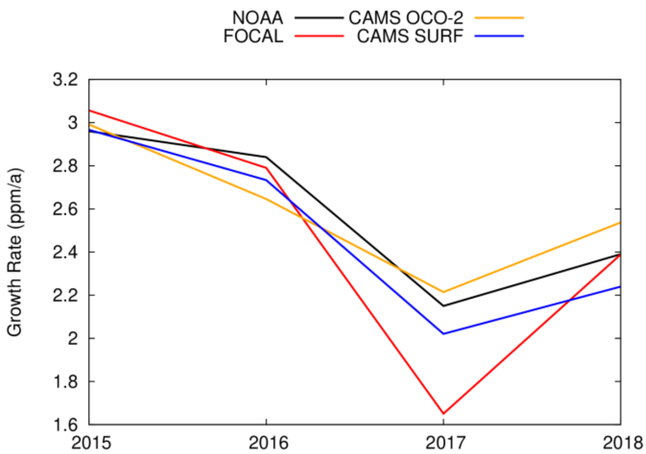

Figure 3. Global annual atmospheric growth rate from NOAA (ftp://aftp.cmdl.noaa.gov/products/trends/co2/co2_gr_gl.txt, accessed 26 February 2020) between years 2015 and 2018, from the 2 CAMS inversions and from CO2_OC2_FOCA.

3.3.3. Maps of annual budgets

Figure 4 displays the maps of the inferred annual budgets of natural CO_2 for the year 2015. As shown already by Chevallier et al. (2019), the two CAMS inversions show rather similar patterns in the northern extra-Tropics, but the ACOS-driven inversion has more spatial gradients than the surface-driven one in the Tropical lands where the surface measurement network is particularly sparse. The CO2_OC2_FOCA inversion has even larger gradients there (Australia excepted), but also in the northern extra-Tropics. The colour bar has actually not been adapted to their variability. Surprisingly, the spatial patterns (irrespective of their amplitude) are similar between the two satellite-driven inversions over land. Over the ocean, the two CAMS inversions are close to each other, but CO2_OC2_FOCA dramatically extends the outgassing regions much.

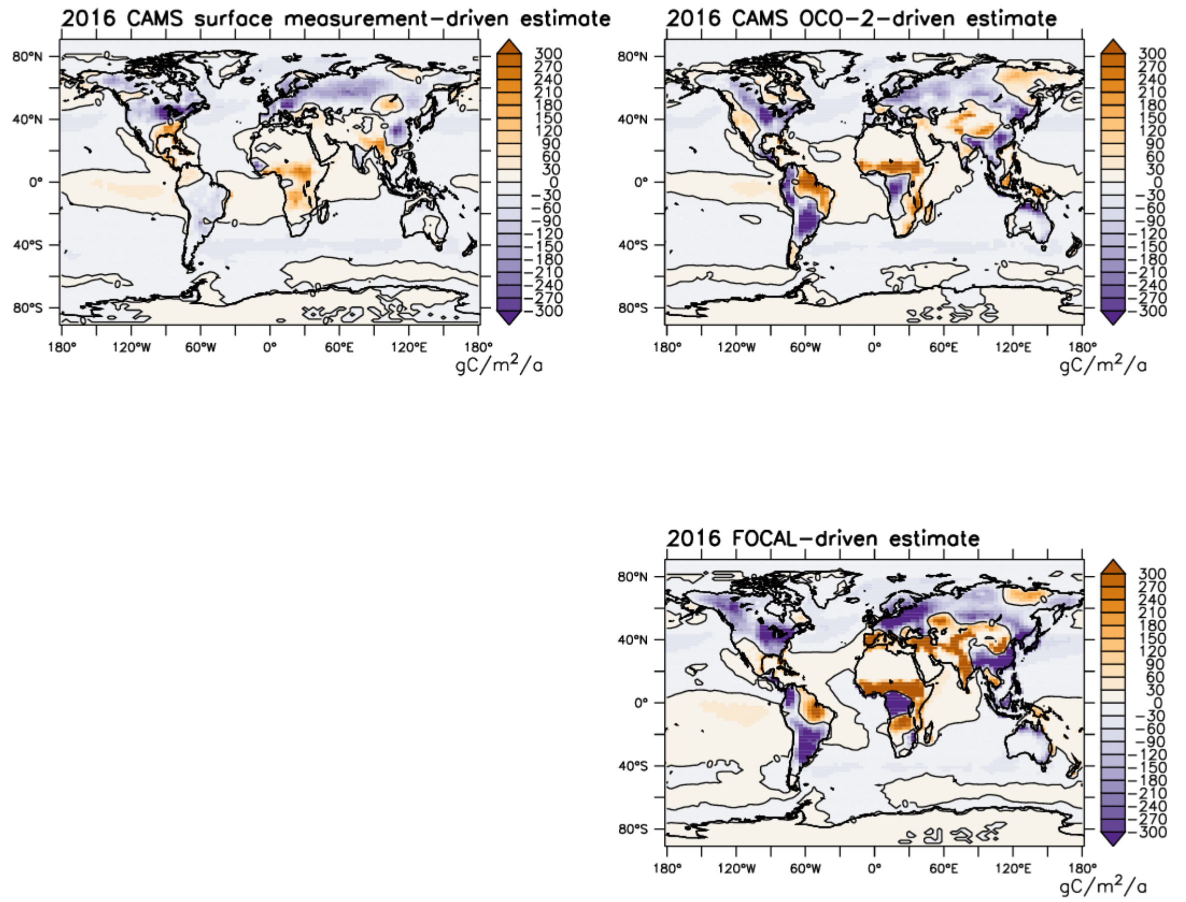

Figure 4. Grid-point budget of the natural CO_2 fluxes for the year 2016 and for the two CAMS inversions and for the CO2_OC2_FOCA product. In the sign convention, positive fluxes correspond to a net carbon source into the atmosphere.

3.3.4. Annual budget time series

The time series of the annual budgets of the inferred natural fluxes at the global or zonal scale are synthesised in Figure 7. The time series of the annual natural carbon budgets at several very broad scales are displayed in Figure 5for the period between 2004 and 2018: the globe, the northern or southern extra-Tropics, and the Tropics with lands and oceans either separated or combined. At the global scale (top row), the curves reflect the growth rate curves of Figure 3, but without the fossil fuel and cement flux component. The three inversions locate the land sink mostly in the northern extra-Tropics, eventhough a large variability is found in the Tropics. The southern extra-Tropical lands (that represent a relatively small surface area) are close to neutral each year. Compared to the two other inversions, the CO2_OC2_FOCA inversion shows larger sinks in the extra-Tropical lands of both hemispheres. Over the oceans, the two CAMS inversions are close to each other North of 25°S, but the Southern Ocean sink reduces when assimilating the ACOS retrievals vs. the surface measurements. With CO2_OC2_FOCA, the northern extra-Tropical uptake and the Tropical outgassing are both enhanced, while the Southern Ocean sink reduces even more than with ACOS.

Detailed results at the scale of the 22 regions of the TransCom 3 experiment (Gurney et al., 2002, Figure 6) are shown in Figure 7 (11 regions over land) and Figure 8 (11 regions over the ocean). The 22 regions together tile the whole globe, apart from the polar ice caps. The two figures show results consistent with the above results, with the CAMS inversions close to each other in most regions and the CO2_OC2_FOCA inversion further away in terms of 4-year value (less so in terms of variability).

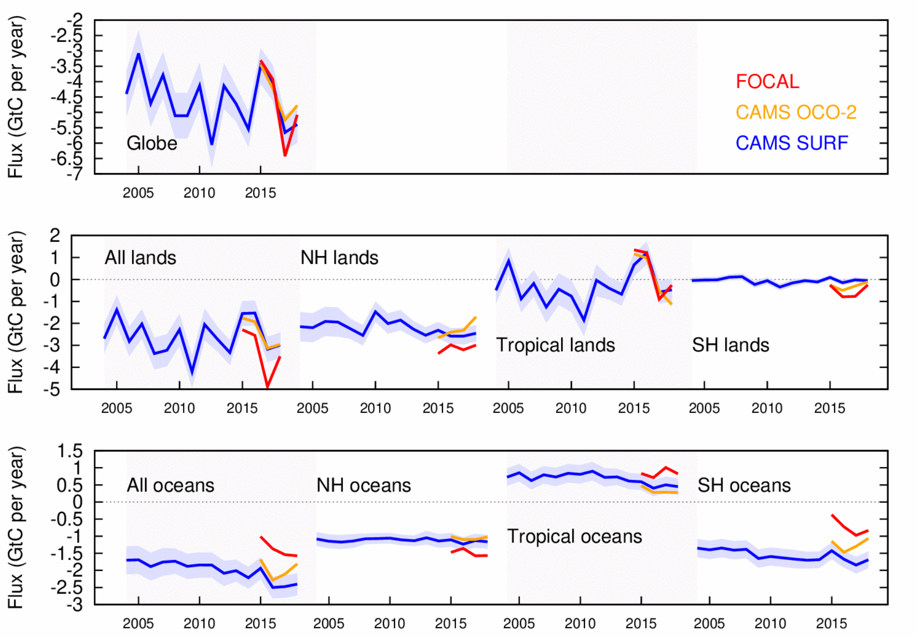

Figure 5. Inferred natural CO_2 annual flux (without fossil fuel emissions) averaged over the globe or over all lands or oceans. In the case of lands and oceans, three broad latitude bands are also

defined: northern extra-Tropics (north of 25°N), Tropics (within 25° of the Equator), and southern extra-Tropics (south of 25°S). The blue curve corresponds to the surface-driven CAMS product with its 1-sigma Bayesian uncertainty. In the sign convention, positive fluxes correspond to a net carbon source into the atmosphere.

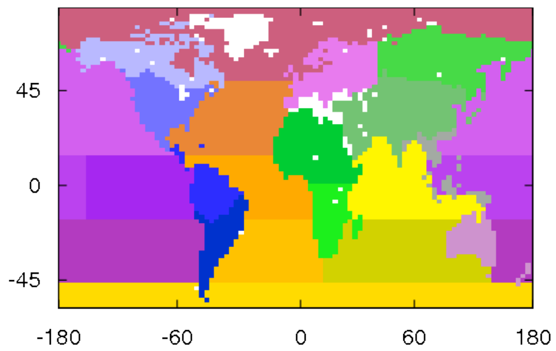

Figure 6. Transcom regions from Gurney et al. (2002).

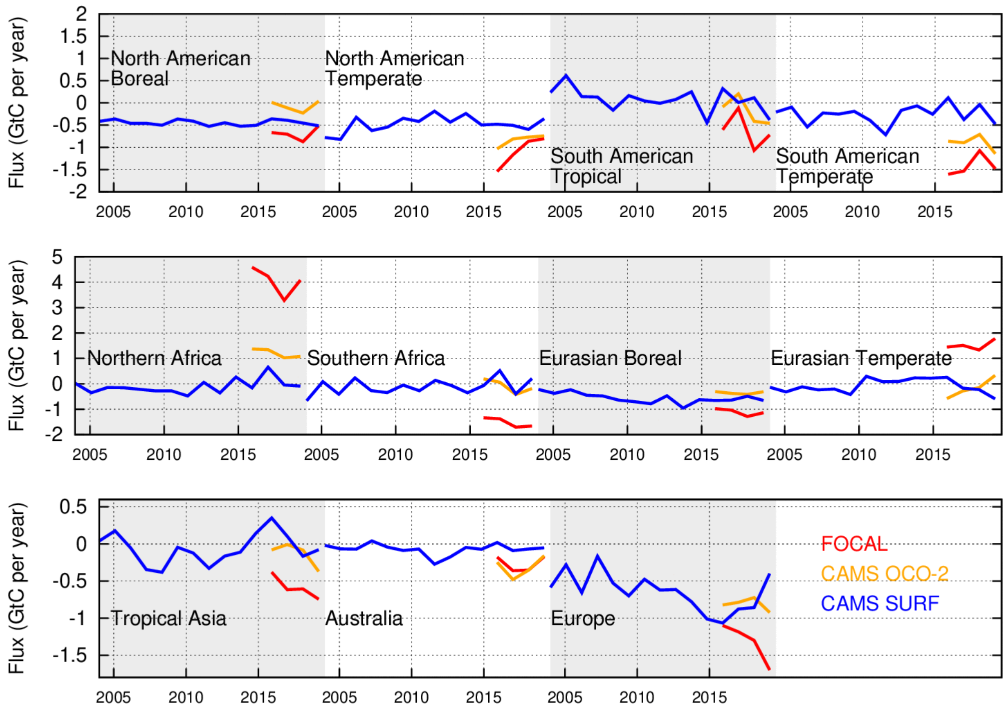

Figure 7. Inferred natural CO_2 annual flux (without fossil fuel emissions) averaged over the TransCom3 land regions. In the sign convention, positive fluxes correspond to a net carbon source into the atmosphere.

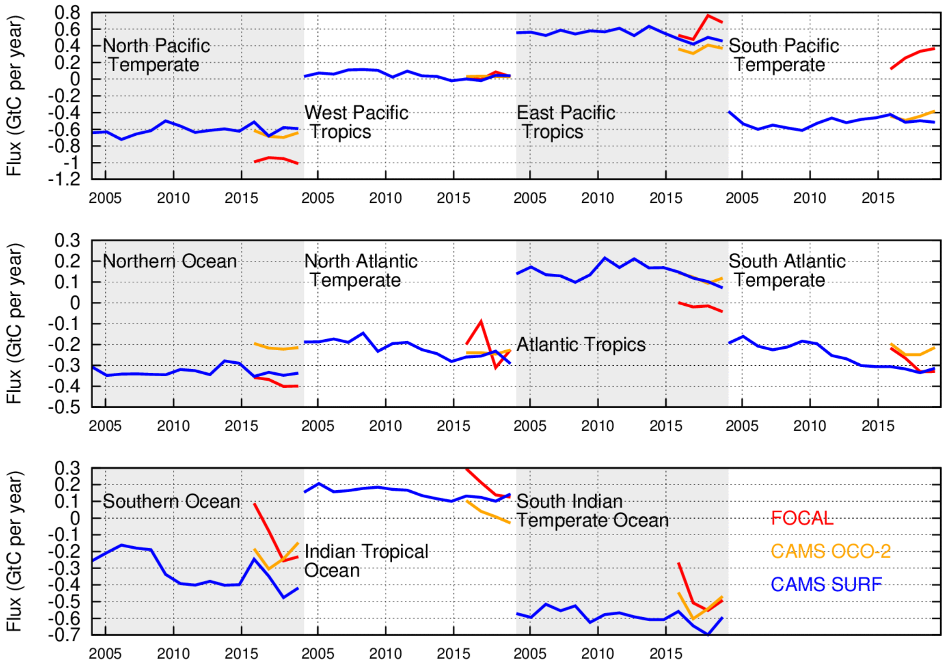

Figure 8. Same as Figure 7, but for the ocean basins.

3.3.5. Differences with aircraft measurements

Following the approach defined in Chevallier et al. (2019), we use continuous and flask dry air mole fraction measurements made by aircraft in the free troposphere to evaluate the three inversions over the CO2_OC2_FOCA period. The free troposphere is simply defined here as the atmospheric layer between 2 and 7 km above sea level (asl). The measurements are all from ObsPack Globalview+ v4.2.1 and NRT v4.4.1 for the period 2015-2018 (Cooperative Global Atmospheric Data Integration Project, 2019, and NOAA Carbon Cycle Group Obspack Team, 2019). We note that no aircraft data is assimilated here. A few outliers for which the difference between model and observation is larger than 40 ppm are rejected: they likely represent very local pollution plumes.

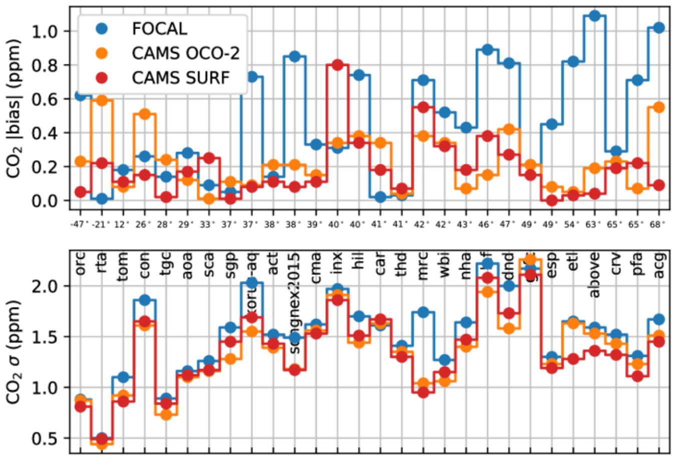

Figure 9. Model-minus-observation absolute differences and standard deviations over the CO2_OC2_FOCA period per measurement program for the CAMS ACOS-based inversion (orange line), the CAMS surface-based inversion (green line) and the CO2_OC2_FOCA-based inversion (blue line). The number of measurement per site, campaign or program varies between 7 (MRC) and 290,361 (ACT). The programs are ranked by increasing mean latitude (North is on the right), irrespective of their latitudinal coverage (which is large of several tens of degrees for ORC, TOM and CON). These mean latitudes are shown in the middle of the panel.

The absolute biases (Figure 9, top) are all less than 1.1 ppm. They are usually even less than 0.4 ppm for the two CAMS inversions, while many values are larger with CO2_OC2_FOCA. There is no obvious latitudinal trend (even when adding the sign of the bias, result not shown), and therefore no obvious flaw of the model vertical mixing (Stephens et al., 2007). Standard deviations vary with the fraction of land masses in a given latitude, as expected. They are about 1.5 ppm in the northern hemisphere for the three inversions, with the CO2_OC2_FOCA-driven numbers larger than the ACOS-driven numbers by ~ 0.2 ppm. When taking all free tropospheric aircraft data together, the posterior simulation deviates from the measurements by -0.1±1.4 ppm (mean bias ± √mean variance across the aircraft programs, irrespective of their number of data), -0.4±1.6 ppm and -0.2±1.4 ppm for the ACOS-driven inversion, for the CO2_OC2_FOCA-driven inversion and for the surface-driven inversion, respectively.

3.3.6. Conclusions

The assimilation of the CO2_OC2_FOCA product in the LSCE global inversion system infers CO2 surface fluxes that are very different from those obtained by the assimilation of surface air-sample measurements. The CO2_OC2_FOCA-driven CO_2 surface fluxes appear to be less credible because (i) the inferred spatial distribution of the ocean outgassing regions is inconsistent with current knowledge of the marine biogeochemistry obtained from sea surface CO2 partial pressure measurements (see the Global ocean surface carbon product of the Copernicus Marine Environment

Monitoring Service[1], (ii) the inferred atmospheric growth rate for year 2017 is notably different from the one seen at marine background stations, (iii) the biases with aircraft data in the free troposphere are larger than when assimilating the surface measurements. In contrast, the ACOS-driven CO_2 surface fluxes (ACOS being restricted to land retrievals here) seem to perform better than the CO2_OC2_FOCA-driven fluxes and even show comparable difference statistics to aircraft measurements in the free troposphere in output to the transport model compared to surface-air-sample-driven fluxes. This result demonstrates that there is no fundamental limitation to atmospheric inverse modelling (e.g., in the realism of the transport model or in the modelled error statistics) when assimilating satellite XCO2 retrievals. The ACOS-driven CO_2 surface fluxes are actually now part of the official CAMS data portfolio.

The various tests performed do not allow us to identify the distinctive asset of ACOS vs. CO2_OC2_FOCA in our system: either the data density (much larger for ACOS over land), the data precision (that seem to be better for ACOS, see 3.2.2), the data trueness (linked both to the quality of the physical retrieval scheme and to its empirical bias-correction), the accuracy of the averaging kernels (see Chevallier, 2015, for a discussion on potential issues with the averaging kernel profiles), or a combination of these qualities at once. Detailed sensitivity tests could be performed for this, but note that our single CO2_OC2_FOCA-driven inversion represented a large computational effort that lasted four weeks on a parallel cluster.

About computational effort, CO2_OC2_FOCA's distinct advantage compared to ACOS is its representation of multiple scattering effects in the radiative transfer in a form that is not costlier than absorption. In preparation for the Copernicus CO2 Monitoring Mission that will provide even larger amount of data than OCO-2 (Pinty et al., 2017), CO2_OC2_FOCA represents an important achievement. In this context and resources permitting, it would be important to document its performance in more detail in order to help prioritize future developments.

4. Assessment of satellite-derived XCH_4 data products

This section is in preparation. It has been delayed because of COVID-19 related issues

[1] http://marine.copernicus.eu/services-portfolio/access-to-products/?option=com_csw&view=details&product_id=MULTIOBS_GLO_BIO_REP_015_005

Acknowledgements

The author thanks M. Reuter and M. Buchwitz for constructive discussions about the use and the evaluation of these products. He is very grateful to the many people involved in the air-sample measurements and in the archiving of these data. Some of the computations of Sections 3.2 and 3.3 have been performed using HPC resources from CCRT under the allocation A0070102201 made by GENCI (Grand Equipement National de Calcul Intensif).

References

Alexe, M., P. Bergamaschi, A. Segers, et al., Inverse modeling of CH_4 emissions for 2010–2011 using different satellite retrieval products from GOSAT and SCIAMACHY, *Atmos. Chem. Phys.*, 15, 113–133, doi:10.5194/acp-15-113-2015, 2015.

Bastos, A., Running, S.W., Gouveia, C. and Trigo, R.M: The global NPP dependence on ENSO: La-Nina and the extraordinary year of 2011. *J. Geophys. Res*. 118, 1247–1255, 2013

Basu, S., Guerlet, S., Butz, A., et al., Global CO_2 fluxes estimated from GOSAT retrievals of total column CO_2, *Atmos. Chem. Phys.*, 13, 8695-8717, 2013.

Basu, S., Krol, M., Butz, A., et al., The seasonal variation of the CO_2 flux over Tropical Asia estimated from GOSAT, CONTRAIL and IASI, *Geophys. Res. Lett.*, doi: 10.1002/2013GL059105, 2014.

Bergamaschi, P., C. Frankenberg, J. F. Meirink, M. Krol, M. G. Villani, S. Houweling, F. Dentener, E. J. Dlugokencky, J. B. Miller, L. V. Gatti, A. Engel, and I. Levin: Inverse modeling of global and regional CH_4 emissions using SCIAMACHY satellite retrievals, *J. Geophys. Res*., 114, doi:10.1029/2009JD012287, 2009.

Bergamaschi, P., et al.: Inverse modeling of European CH_4 emissions 2001-2006, *J. Geophys. Res*., 115(D22309), doi:10.1029/2010JD014180, 2010.

Bergamaschi, P., S. Houweling, A. Segers, M. Krol, C. Frankenberg, R. A. Scheepmaker, E. Dlugokencky, S. Wofsy, E. Kort, C. Sweeney, T. Schuck, C. Brenninkmeijer, H. Chen, V. Beck and C. Gerbig, Atmospheric CH_4 in the first decade of the 21st century: Inverse modeling analysis using SCIAMACHY satellite retrievals and NOAA surface measurements, *J. Geophys. Res*., 118, doi:10.1002/jgrd.50480, 2013.

Bloom, A. A., Palmer, P. I., Fraser, A., and Reay, D. S.: Seasonal variability of tropical wetland CH4 emissions: the role of the methanogen-available carbon pool, *Biogeosciences*, 9, 2821–2830, doi:10.5194/bg-9-2821-2012, 2012

Boden, T. A., Marland, G., and Andres, R. J.: Global, regional, and national fossil-fuel CO2 emissions. Carbon Dioxide Information Analysis Center, Oak Ridge National Laboratory, U.S. Department of Energy, Oak Ridge, Tenn., U.S.A., Doi:10.3334/CDIAC/00001_V2013, 2013

Buchwitz, M., M. Reuter, O. Schneising, et al., The Greenhouse Gas Climate Change Initiative (GHG-CCI): comparison and quality assessment of near-surface-sensitive satellite-derived CO_2 and CH_4 global data sets, *Remote Sensing of Environment*, 162, 344–362, doi:10.1016/j.rse.2013.04.024, 2015.

Buchwitz, M., Dils, B., Boesch, H., et al., Product Validation and Intercomparison Report (PVIR) for the GHG-CCI project of ESA's Climate Change Initiative, version 3.1 (PVIRv4), 24 February 2016, 2016.

Buchwitz, M., Dils, B., Boesch, H., et al., Product Validation and Intercomparison Report (PVIR) for the for the Essential Climate Variable (ECV) Greenhouse Gases (GHG) for data set Climate Research Data Package No. 4 (CRDP#4), 9 February 2017, 2017a.

Buchwitz, M., M. Reuter, O. Schneising, W. Hewson, R.G. Detmers, H. Boesch, O.P. Hasekamp, I. Aben, H. Bovensmann, J.P. Burrows, A. Butz, F. Chevallier, B. Dils, C. Frankenberg, J. Heymann, G. Lichtenberg, M. De Mazière, J. Notholt, R. Parker, T. Warneke, C. Zehner, D.W.T. Griffith, N.M. Deutscher, A. Kuze, H. Suto, D. Wunch, 2017: Global satellite observations of column-averaged carbon dioxide and methane: The GHG-CCI XCO2 and XCH4 CRDP3 data set, Remote Sensing of Environment, doi: 10.1016/j.rse.2016.12.027, accepted, 2017b.

Buchwitz, M., Dils, B., Reuter, M., Boesch, H., Aben, I., Product Validation and Intercomparison Report (PVIR) for the for the Essential Climate Variable (ECV) Greenhouse Gases (GHG): XCO_2 and/or XCH_4 from OCO-2, TanSat, Sentinel-5-Precursor and GOSAT-2, 17 February 2020, 2020.

Butz, A., Guerlet, S., Hasekamp, O., et al., Toward accurate CO_2 and CH_4 observations from GOSAT, *Geophys. Res. Lett.*, doi:10.1029/2011GL047888, 2011.

Canadell, J. G., Ciais, P., Dhakal, S., et al., Interactions of the carbon cycle, human activity, and the climate system: a research portfolio, *Curr. Opin. Environ. Sustainabil.*, 2, 301–311, 2010.

Chevallier, F., et al.: Inferring CO_2 sources and sinks from satellite observations: method and application to TOVS data. *J. Geophys. Res.*, 110, D24309, 2005.

Chevallier, F.: Impact of correlated observation errors on inverted CO2 surface fluxes from OCO measurements, *Geophys. Res. Lett.*, 34, L24804, doi:10.1029/2007GL030463, 2007.

Chevallier, F., Maksyutov, S., Bousquet, P., Bréon, F.-M., Saito, R., Yoshida, Y., and Yokota, T.: On the accuracy of the CO_2 surface fluxes to be estimated from the GOSAT observations. *Geophys. Res. Lett.*, 36, L19807, doi:10.1029/2009GL040108, 2009.

Chevallier, F., et al.: CO_2 surface fluxes at grid point scale estimated from a global 21-year reanalysis of atmospheric measurements. *J. Geophys. Res.*, 115, D21307, doi:10.1029/2010JD013887, 2010a.

Chevallier, F., Feng, L., Boesch, H., Palmer, P., and Rayner, P.: On the impact of transport model errors for the estimation of CO_2 surface fluxes from GOSAT observations. *Geophys. Res. Lett.*, 37, L21803, doi:10.1029/2010GL044652, 2010b.

Chevallier, F., Deutscher, N. M., Conway, T. J., Ciais, P., Ciattaglia, L., Dohe, S., Frohlich, M., Gomez-Pelaez, A. J., Griffith, D., Hase, F., Haszpra, L., Krummel, P., Kyro, E., Labuschagne, C., Langenfelds, R., Machida, T., Maignan, F., Matsueda, H., Morino, I., Notholt, J., Ramonet, M., Sawa, Y., Schmidt, M., Sherlock, V., Steele, P., Strong, K., Sussmann, R., Wennberg, P., Wofsy, S., Worthy, D., Wunch, D., and Zimnoch, M.: Global CO_2 fluxes inferred from surface air-sample measurements and from TCCON retrievals of the CO_2 total column, *Geophys. Res. Lett.*, 38, L24810, doi:10.1029/2011GL049899, 2011

Chevallier, F., Bergamaschi, P., Kaminiski, T., Scholze, M., Climate Assessment Report (CAR) for the GHG-CCI project of ESA's Climate Change Initiative, version 1.1 (CARv1.1), 18. Nov. 2013, 2013.

Chevallier, F., and O'Dell, C. W., Error statistics of Bayesian CO_2 flux inversion schemes as seen from GOSAT, *Geophys. Res. Lett.*, doi: 10.1002/grl.50228, 2013.

Chevallier, F., Palmer, P.I., Feng, L., Boesch, H., O'Dell, C.W., Bousquet, P., Towards robust and consistent regional CO_2 flux estimates from in situ and space-borne measurements of atmospheric CO_2, *Geophys. Res. Lett.*, 41, 1065-1070, DOI: 10.1002/2013GL058772, 2014a.

Chevallier, F., Buchwitz, M., Bergamaschi, et al., User Requirements Document for the GHG-CCI project of ESA's Climate Change Initiative, version 2 (URDv2), 28. August 2014, 2014b.

Chevallier, F.: On the statistical optimality of CO_2 atmospheric inversions assimilating CO_2 column retrievals, Atmos. Chem. Phys., 15, 11133–11145, https://doi.org/10.5194/acp-15-11133-2015, 2015.

Chevallier, F., P. Bergamaschi, D. Brunner, S. Gonzi, S. Houweling, T. Kaminski, G. Kuhlmann, T. T. van Leeuwen, J. Marshall, P. I. Palmer, and M. Scholze, Climate Assessment Report for the GHG-CCI project of ESA's Climate Change Initiative, pp. 87, version 2, 22 April 2015, 2015.

Chevallier, F., M. Alexe, P. Bergamaschi, D. Brunner, L. Feng, S. Houweling, T. Kaminski, W. Knorr, T. T. van Leeuwen, J. Marshall, P. I. Palmer, M. Scholze, A.-M. Sundström and M. Voßbeck, Climate Assessment Report for the GHG-CCI project of ESA's Climate Change Initiative, pp. 94, version 3, 3 May 2016, 2016.

Chevallier, F., P. Bergamaschi, D. Brunner, L. Feng, S. Houweling, T. Kaminski, W. Knorr, J. Marshall, P. I. Palmer, S. Pandey, M. Reuter, M. Scholze, and M. Voßbeck, Climate Assessment Report for the GHG-CCI project of ESA's Climate Change Initiative, pp. 96, version 4, http://cci.esa.int/sites/default/files/GHG-CCI_CARv4_final.pdf, 27 March 2017, 2017.

Chevallier, F., Validation report for the inverted CO_2 fluxes, v18r3. CAMS deliverable CAMS73_2018SC1_ D73.1.4.1-2018-v2_201911. http://atmosphere.copernicus.eu/, 2019.

Chevallier, F., Remaud, M., O'Dell, C. W., Baker, D., Peylin, P., and Cozic, A.: Objective evaluation of surface- and satellite-driven carbon dioxide atmospheric inversions, Atmos. Chem. Phys., 19, 14233–14251, https://doi.org/10.5194/acp-19-14233-2019, 2019.

Cogan, A. J., Boesch, H., Parker, R. J., et al., Atmospheric carbon dioxide retrieved from the Greenhouse gases Observing SATellite (GOSAT): Comparison with ground-based TCCON observations and GEOS-Chem model calculations, *J. Geophys. Res.*, 117, D21301, doi:10.1029/2012JD018087, 2012.

Conway, T. J., Tans, P. P., Waterman, L. S., Thoning, K. W., Kitzis, D. R., Masarie, K. A. and Zhang, N.: Evidence for interannual variability of the carbon cycle from the National Oceanic and Atmospheric Administration/Climate Monitoring and Diagnostics Laboratory Global Air Sampling Network, *J. Geophys. Res*., 99(D11), 22,831–22,855, doi:10.1029/94JD01951, 1994

Cramer, W., Kicklighter, D. W., Bondeau, A., Iii, B. M., Churkina, G., Nemry, B., Ruimy, A., Schloss, A. L. and Intercomparison, ThE. P. OF. ThE. P. NpP. M., Comparing global models of terrestrial net primary productivity (NPP): overview and key results. *Global Change Biology*, 5: 1–15. doi:10.1046/j.1365-2486.1999.00009.x, 1999.

Cressot, C., F. Chevallier, P. Bousquet, et al., On the consistency between global and regional methane emissions inferred from SCIAMACHY, TANSO-FTS, IASI and surface measurements, *Atmos. Chem. Phys.*, 14, 577-592, 2014.

Cressot, C., Pison, I., Rayner, P. J., Bousquet, P., Fortems-Cheiney, A., and Chevallier, F.: Can we detect regional methane anomalies? A comparison between three observing systems, Atmos. Chem. Phys., 16, 9089-9108, doi:10.5194/acp-16-9089-2016, 2016..

Crevoisier, C., Sweeney, C., Gloor, M., Sarmiento, J. L., and Tans, P. P.: Regional U.S. carbon sinks from three-dimensional atmospheric CO_2 sampling, *Proc. Natl. Acad. Sci.* (2010), 107: 18348-18353, 2010.

Crowell, S., Baker, D., Schuh, A., Basu, S., Jacobson, A. R., Chevallier, F., Liu, J., Deng, F., Feng, L., McKain, K., Chatterjee, A., Miller, J. B., Stephens, B. B., Eldering, A., Crisp, D., Schimel, D., Nassar, R., O'Dell, C. W., Oda, T., Sweeney, C., Palmer, P. I., and Jones, D. B. A.: The 2015–2016 carbon cycle as seen from OCO-2 and the global in situ network, Atmos. Chem. Phys., 19, 9797–9831, https://doi.org/10.5194/acp-19-9797-2019, 2019.

Dee, D. P., et al., The ERA-Interim reanalysis: configuration and performance of the data assimilation system, Q. J. R. Meteorol. Soc., 137, 553–597, 2011.

Desroziers G., Berre, L., Chapnik, B., and Poli, P.: Diagnosis of observation, background and analysis error statistics in observation space. *Q. J. Roy. Meteor. Soc.*, 131, 3385-3396, 2005.

Detmers, R., Hasekamp, O., Aben, I., Houweling, S., van Leeuwen, T.T., Butz, A., Landgraf, J., Kohler, P., Guanter, L., and Poulter, B.: Anomalous carbon uptake in Australia as seen by GOSAT. *Geophysical Research Letters*, 42(19), 2015

Dlugokencky, E. J., L. P. Steele, P. M. Lang, and K. A. Masarie, The growth rate and distribution of atmospheric methane, *J. Geophys. Res.*, 99, 17021–17043. 1994.

Dlugokencky, E. J., S. Houweling, L. Bruhwiler, K. A. Masarie, P.M. Lang, J. B. Miller, and P. P. Tans, Atmospheric methane levels off: Temporary pause or a new steady-state? *Geophys. Res. Lett.*, 30(19), 1992, doi:10.1029/2003GL018126, 2003.

Dlugokencky, E. J., Bruhwiler, L., White, J. W. C., et al., Observational constraints on recent increases in the atmospheric CH_4 burden, *Geophys. Res. Lett.*, 36, L18803, doi:10.1029/2009GL039780, 2009.

Dlugokencky, E., P. Lang, J. Mund, A. Crotwell, M. Crotwell, and K. Thoning, Atmospheric carbon dioxide dry air mole fractions from the NOAA ESRL carbon cycle cooperative global air sampling network, 1968-2015, 2016.

Dubovik, O. and King, M. D.: A flexible inversion algorithm for retrieval of aerosol optical properties from Sun and sky radiance measurements, *J. Geophys. Res.*, 105, 20673–20696, 2000.

Enting, I. G.: Inverse Problems in Atmospheric Constituent Transport. Cambridge University Press, 2002.

ESA: A-SCOPE - Advanced Space Carbon And Climate Observation of Planet Earth, Technical Report SP-1313/1, European Space Agency, Noordwijk, The Netherlands. 2008

Feng, L., Palmer, P. I., Bösch, H., and Dance, S.: Estimating surface CO_2 fluxes from space-borne CO_2 dry air mole fraction observations using an ensemble Kalman Filter, *Atmos. Chem. Phys.*, 9, 2619–2633, doi:10.5194/acp-9-2619-2009, 2009.

Feng, L., P. I. Palmer, R. J. Parker, et al., Estimates of European uptake of CO_2 inferred from GOSAT X_{CO2} retrievals: sensitivity to measurement bias inside and outside Europe, *Atmos. Chem. Phys.*, 16, 1289-1302, doi:10.5194/acp-16-1289-2016, 2016a.

Feng, L., Palmer, P. I., Bösch, H., Parker, R. J., Webb, A. J., Correia, C. S. C., Deutscher, N. M., Domingues, L. G., Feist, D. G., Gatti, L. V., Gloor, E., Hase, F., Kivi, R., Liu, Y., Miller, J. B., Morino, I., Sussmann, R., Strong, K., Uchino, O., Wang, J., and Zahn, A.: Consistent regional fluxes of CH4 and CO2 inferred from GOSAT proxy XCH4:XCO2 retrievals, 2010–2014, Atmos. Chem. Phys. Discuss., doi:10.5194/acp-2016-868, in review, 2016b.Frankenberg, C., Aben, I., Bergamaschi, P., et al., Global column-averaged methane mixing ratios from 2003 to 2009 as derived from SCIAMACHY: Trends and variability, *J. Geophys. Res.*, doi:10.1029/2010JD014849, 2011.

Frankenberg, C., Product User Guide (PUG) for the IMAP-DOAS XCH4 SCIAMACHY Data Products, version 1, ESA Climate Change Initiative (CCI) GHG-CCI project, 13 Dec. 2012, 2012.

Fraser, A., Palmer, P. I., Feng, L., et al., Estimating regional methane surface fluxes: the relative importance of surface and GOSAT mole fraction measurements, *Atmos. Chem. Phys.*, 13, 5697-5713, doi:10.5194/acp-13-5697-2013, 2013.

Fraser, A., Palmer, P. I., Feng, L. et al., Estimating regional fluxes of CO_2 and CH_4 using space-borne observations of XCH_4:XCO_2, *Atmos. Chem. Phys.*, 14, 12883-12895, doi:10.5194/acp-14-12883-2014, 2014.

Friedl, M. A., Strahler, A. H., and Hodges, J.: ISLSCP II MODIS (Collection 4) IGBP Land Cover, 2000–2001, in: ISLSCP Initia- tive II Collection, Data set, edited by: Hall, F. G., Collatz, G., Meeson, B., Los, S., Brown de Colstoun, E., and Landis, D., Oak Ridge National Laboratory Distributed Active Archive Cen- ter, Oak Ridge, Tennessee, USA, doi:10.3334/ORNLDAAC/96

Gatti, L. V., Gloor, M., Miller, J. B., Doughty, C. E., Malhi, Y., Domingues, L. G., Basso, L. S., Martinewski, A., Correia, C. S. C., Borges, V. F., Freitas, S., Braz, R., Anderson, L. O., Rocha, H., Grace, J., Philips, O. L, and Lloyd, J.: Drought sensitivity of Amazonian carbon balance revealed by atmospheric measurements, *Nature*, 506(7486), 76-80, doi:10.1038/nature12957, 2014

Giles, D.M., Holben, B.N., Eck, T.F., Sinyuk, A., Smirnov, A., Slutsker, I., Dickerson, R. R., Thompson, A.M., and Shafer J. S.: An analysis of AERONET aerosol absorption properties and classifications representative of aerosol source regions, J. Geophys. Res., 117, D17203, 2012.

GLOBALVIEW-CO2: Cooperative Global Atmospheric Data Integration Project. 2013, updated annually. Multi-laboratory compilation of synchronized and gap-filled atmospheric carbon dioxide records for the period 1979-2012 (obspack_co2_1_GLOBALVIEW-CO2_2013_v1.0.4_2013-12-23). Compiled by NOAA Global Monitoring Division: Boulder, Colorado, U.S.A. Data product accessed at http://dx.doi.org/10.3334/OBSPACK/1002. 2013

Gerbig, C., Lin, J. C., Wofsy, S. C., Daube, B. C., Andrews, A. E., Stephens, B. B., Bakwin, P. S., and Grainger, C. A.: Toward constraining regional-scale fluxes of CO2 with atmospheric observations over a continent: 2. Analysis of COBRA data using a receptor-oriented framework, J. Geophys. Res.-Atmos., 108, 4757, doi:10.1029/2003JD003770, 2003.

Guerlet, S., Basu, S., Butz, A., et al., Reduced carbon uptake during the 2010 Northern Hemisphere summer from GOSAT, *Geophys. Res. Lett.*, doi: 10.1002/grl.50402, 2013a.

Guerlet, S., Butz, A., Scheppers, D., Basu, S., Hasekamp, O.P., Kuze, A., Yokota, T., Blavier, J.-F., Deutcher, N.M., Griffith, D.W.T, Hase, F., Kyrö, E., Morino, I, Scherlock, V., Sussmann, R., Galli, A., and Aben, I.: Impact of aerosol and thin cirrus on retrieving and validating XCO_2 from GOSAT shortwave infrared measurements. *J. Geophys. Res*., 118, 4887-4905, 2013b.

Gurney, K.R., et al.: Towards robust regional estimates of CO_2 sources and sinks using atmospheric transport models. *Nature*, 415:6872, 626-630, 2002.

Harris, I., Jones, P.D., Osborn, T.J. and Lister, D.H., Updated high-resolution grids of monthly climatic observations – the CRU TS3.10 Dataset. *Int. J. Climatol.*. doi: 10.1002/joc.3711, 2013

Haverd, V., Raupach, M. R., Briggs, P. R., J. G. Canadell., Davis, S. J., Law, R. M., Meyer, C. P., Peters, G. P., Pickett-Heaps, C., and Sherman, B.: The Australian terrestrial carbon budget, *Biogeosciences*, 10, 851-869, doi:10.5194/bg-10-851-2013, 2013.

Hayman, G. D., O'Connor, F. M., Dalvi, et al., Comparison of the HadGEM2 climate-chemistry model against in-situ and SCIAMACHY atmospheric methane data, *Atmos. Chem. Phys.*, 14, 13257-13280, doi:10.5194/acp-14-13257-2014, 2014.

Heimann, M.: The global atmospheric tracer model TM2, Technical Report No. 10, Max-Planck-Institut für Meteorologie, Hamburg, Germany. 1995

Heimann, M., G. Esser, A. Haxeltine, J. Kaduk, D.W. Kicklighter, W. Knorr, G. H. Kohlmaier, A. D. McGuire, J. Melillo, B. Moore, et al., Evaluation of terrestrial carbon cycle models through simulations of the seasonal cycle of atmospheric CO2: First results of a model intercomparison study, Global Biogeochemical Cycles, 12, 1–24, 1998.

Heimann, M. and S. Körner: The global atmospheric tracer model TM3. In: Max-Planck-Institut für Biogeochemie (Eds.): Technical Report. Vol. 5. Max-Planck-Institut für Biogeochemie, Jena. pp. 131, 2003.

Hewson, W.: ESA Climate Change Initiative (CCI) Product User Guide: University of Leicester full-physics XCO2 retrieval algorithm for CRDP3–OCFPv6.0 for the Essential Climate Variable (ECV): Greenhouse Gases (GHG), Version 3, 25 February 2016, 2016.

Heymann, J., Schneising, O., Reuter, M., et al., SCIAMACHY WFM-DOAS XCO_2: comparison with CarbonTracker XCO_2 focusing on aerosols and thin clouds, *Atmos. Meas. Tech.*, 5, 1935-1952, 2012.

Holben, B., Eck, T. F., Slutsker, I., Tanre, D., Buis, J. P., Setzer, A., Vermote, E., Reagan, J. A., Kaufman, Y. J., Nakajima, T., Lavenu, F., Jankowiak, I., and Smirnov, A.: AERONET – A Federated Instrument Network and Data Archive for Aerosol Characterization, *Remote Sens. Environ.*, 66, 1–16, 1998.

Hourdin, F., et al.: The LMDZ4 general circulation model: climate performance and sensitivity to parametrized physics with emphasis on tropical convection, *Climate Dynamics*, 27, 787-813, doi:10.1007/s00382-006-0158-0, 2006.

Houweling, S., et al.: The importance of transport model uncertainties for the estimation of CO_2 sources and sinks using satellite measurements. *Atmos. Chem. Phys.*, 10, 9981-9992, doi:10.5194/acp-10-9981-2010, 2010.

Houweling, S., M. Krol, P. Bergamaschi, C. Frankenberg, E. J. Dlugokencky, I. Morino, J. Notholt, V. Sherlock, D. Wunch, V. Beck, C. Gerbig, H. Chen, E. A. Kort, T. Röckmann and I. Aben, A multi-year methane inversion using SCIAMACHY, accounting for systematic errors using TCCON measurements, *Atmos. Chem. Phys.*, 14, 3991–4012, doi:10.5194/acp-14-3991-2014, 2014.

Houweling, S., D. Baker, S. Basu, H. Boesch, A. Butz, F. Chevallier, F. Deng, E. Dlugockencky, L. Feng, A. Ganshin, O. P. Hasekamp, D. Jones, S. Maksyutov, J. Marshall, T. Oda, C. O'Dell, S. Oshchepkov, P. Paul, P. Peylin, Z. Poussi, F. Reum, H. Takagi, Y. Yoshida, R. Zhuravlev, An inter-comparison of inverse models for estimating sources and sinks of CO_2 using GOSAT measurements. *J. Geophys. Res. Atmos.*, 120, 5253–5266, doi:10.1002/2014JD022962, 2015.

Jacobson, A. R., Fletcher, S. E. M., Gruber, N., Sarmiento, J. L., and Gloor, M.: A joint atmosphere-ocean inversion for surface fluxes of carbon dioxide: 1. Methods and global-scale fluxes, *Global Biogeochem. Cy.*, 21(1), GB1020, doi:10.1029/2006GB002703, 2007.

Jung, M., et al.: Global patterns of land-atmosphere fluxes of carbon dioxide, latent heat, and sensible heat derived from eddy covariance, satellite, and meteorological observations, *J. Geophys. Res.*, 116, G00J07, doi:10.1029/2010JG001566. 2011.

Keeling, C., S. Piper, and Scripps Institution of Oceanography, Exchanges of Atmospheric CO2 and 13CO2 with the Terrestrial Biosphere and Oceans from 1978 to 2000, SIO reference, Scripps Institution of Oceanography, University of California, San Diego, 2001.

Kicklighter, D. W., Bondeau, A., Schloss, A. L., Kaduk, J., Mcguire, A. D. et al., Comparing global models of terrestrial net primary productivity (NPP): global pattern and differentiation by major biomes. *Global Change Biology*, 5: 16–24. doi:10.1046/j.1365-2486.1999.00003.x, 1999.

Kirschke, S., Bousquet, P., Ciais, P., et al., Three decades of global methane sources and sinks, *Nat. Geosci.*, 6, 813–823, doi:10.1038/ngeo1955, 2013.

Kort, E. A., Frankenberg, C., Costigan, K. R., et al., Four corners: The largest US methane anomaly viewed from space, *Geophys. Res. Lett.*, 41, doi:10.1002/2014GL061503, 2014.

Krol, M. C., S. Houweling, B. Bregman, M. van den Broek, A. Segers, P. van Velthoven, W. Peters, F. Dentener, and P. Bergamaschi, The two-way nested global chemistry-transport zoom model TM5: algorithm and applications, *Atmos. Chem. Phys.*, 5, 417-432, 2005.

Lindqvist, H., C. W. O'Dell, S. Basu, H. Boesch, F. Chevallier, N. Deutscher, L. Feng, B. Fisher, F. Hase, M. Inoue, R. Kivi, I. Morino, P. I. Palmer, R. Parker, M. Schneider, R. Sussmann, and Y. Yoshida, Does GOSAT capture the true seasonal cycle of carbon dioxide?, *Atmos. Chem. Phys*., 15, 13023-13040, doi:10.5194/acp-15-13023-2015, 2015.

Ma, X., A. Huete, J. Cleverly, D. Eamus, F. Chevallier, J. Joiner, B. Poulter, Y. Zhang, L. Guanter, W. Meyer, Z. Xie, G. Ponce-Campos: Drought rapidly disseminates the 2011 large CO_2 uptake in semi-arid Australia. Scientific Reports, 6. doi: 10.1038/srep37747, 2016.

Mäder, J. A., J. Staehelin, D. Brunner, W. A. Stahel, I. Wohltmann, and T. Peter, Statistical modeling of total ozone: Selection of appropriate explanatory variables, *J. Geophys. Res*., 112, D11108, doi:10.1029/2006JD007694, 2007.

Meirink, J. F., P. Bergamaschi, and M. Krol: Four-dimensional variational data assimilation for inverse modelling of atmospheric methane emissions: Method and comparison with synthesis inversion, *Atmos. Chem. Phys.*, 8, 6341–6353, 2008.

Mikaloff Fletcher, S. E., Gruber, N., Jacobson, A. R., Doney, S. C., Dutkiewicz, S., and co-authors: Inverse estimates of anthropogenic CO2 uptake, transport, and storage by the ocean, *Global Biogeochem. Cy*., 20(2), GB2002, doi:10.1029/2005GB002530, 2006.

Mikaloff Fletcher, S. E., Gruber, N., Jacobson, A. R., Gloor, M., Doney, S. C., and co-authors: Inverse estimates of the oceanic sources and sinks of natural CO2 and the implied oceanic carbon transport, *Global Biogeochem. Cy*., 21(1), GB1010, doi:10.1029/2006GB002751, 2007.

Monteil, G., Houweling, S., Butz, A., et al., Comparison of CH_4 inversions based on 15 months of GOSAT and SCIAMACHY observations, *J. Geophy. Res.*, doi: 10.1002/2013JD019760, Vol 118, Issue 20, 11807-11823, 2013.

Notholt, J., et al.: Product Validation and Intercomparison Report (PVIR), ESA Climate Change Initiative (CCI) GHG-CCI project, v2.0, 4 Nov. 2013, 2013.

O'Dell, C. W., Connor, B., Bösch, H., O'Brien, D., Frankenberg, C., Castano, R., Christi, M., Eldering, D., Fisher, B., Gunson, M., McDuffie, J., Miller, C. E., Natraj, V., Oyafuso, F., Polonsky, I., Smyth, M., Taylor, T., Toon, G. C., Wennberg, P. O., and Wunch, D.: The ACOS CO2 retrieval algorithm – Part 1: Description and validation against synthetic observations, *Atmos. Meas. Tech*., 5, 99–121, doi:10.5194/amt-5-99-2012, 2012.

O'Dell, C. W., Eldering, A., Wennberg, P. O., Crisp, D., Gunson, M. R., Fisher, B., Frankenberg, C., Kiel, M., Lindqvist, H., Mandrake, L., Merrelli, A., Natraj, V., Nelson, R. R., Osterman, G. B., Payne, V. H., Taylor, T. E., Wunch, D., Drouin, B. J., Oyafuso, F., Chang, A., McDuffie, J., Smyth, M., Baker, D. F., Basu, S., Chevallier, F., Crowell, S. M. R., Feng, L., Palmer, P. I., Dubey, M., García, O. E., Griffith, D. W. T., Hase, F., Iraci, L. T., Kivi, R., Morino, I., Notholt, J., Ohyama, H., Petri, C., Roehl, C. M., Sha, M. K., Strong, K., Sussmann, R., Te, Y., Uchino, O., and Velazco, V. A.: Improved retrievals of carbon dioxide from Orbiting Carbon Observatory-2 with the version 8 ACOS algorithm, Atmos. Meas. Tech., 11, 6539–6576, https://doi.org/10.5194/amt-11-6539-2018, 2018.

O'Neill, N. T.,T. F., Eck, A. Smirnov, B. N.Holben, S. Thulasiraman, Spectral discrimination of coarse and fine mode optical depth, *J. Geophys. Res*., 108, D17, 4559-4573, doi:10.1029/2002JD002975, 2003.

Oda, T., and Maksyutov, S.: A very high-resolution (1 km×1 km) global fossil fuel CO2 emission inventory derived using a point source database and satellite observations of nighttime lights, *Atmos. Chem. Phys*., 11, 543–556, doi:10.5194/acp-11-543-2011, 2011.

Olivier, J. G. J., van Aardenne, J. A., Dentener, F., Ganzeveld, L., and Peters, J. A. H. W.: Recent trends in global greenhouse gas emissions: regional trends and spatial distribution of key sources, in: Non-CO2 Greenhouse Gases (NCGG-4), edited by: van Amstel, A., Millpress, Rotterdam, 325–330, 2005.

Olivier, J. G. J., Janssens-Maenhout, G., and Peters, J. A. H. W., Trends in global CO_2 emissions, 2012 Report, PBL Netherlands Environmental Assessment Agency, The Hague, Joint Research Centre, Ispra, ISBN 978-92-79-25381-2, 2012.

Olsen, S. C. and Randerson, J. T.: Differences between surface and column atmospheric CO_2 and implications for carbon cycle research, *J. Geophys. Res*., 109, D02301, doi:10.1029/2003JD003968, 2004.

Oshchepkov, S., A. Bril, T. Yokota, et al., Effects of atmospheric light scattering on spectroscopic observations of greenhouse gases from space. Part 2: Algorithm intercomparison in the GOSAT data processing for CO_2 retrievals over TCCON sites, *J. Geophys. Res.*, 118, 1493–1512, doi:10.1002/jgrd.50146, 2013.

Pan, Y., et al.: A large and persistent carbon sink in the world's forests, Science, 333, 988–993, 2011.

Pandey, S., Houweling, S., Krol, M., Aben, I., Chevallier, F., Dlugokencky, E. J., Gatti, L. V., Gloor, M., Miller, J. B., Detmers, R., Machida, T., and Röckmann, T.: Inverse modeling of GOSAT-retrieved ratios of total column CH_4 and CO_2 for 2009 and 2010, *Atmos. Chem. Phys. Discuss.*, doi:10.5194/acp-2016-77, in review, 2016.

Parazoo, N. C., Bowman, K., Frankenberg, C., et al., Interpreting seasonal changes in the carbon balance of southern Amazonia using measurements of XCO_2 and chlorophyll fluorescence from GOSAT, *Geophys. Res. Lett.*, 40, 2829–2833, doi:10.1002/grl.50452, 2013.

Parker, R., Boesch, H., Cogan, A., et al., Methane Observations from the Greenhouse gases Observing SATellite: Comparison to ground-based TCCON data and Model Calculations, *Geophys. Res. Lett.*, doi:10.1029/2011GL047871, 2011.

Peters, W., Jacobson, A. R., Sweeney, C., et al.: An atmospheric perspective on North American carbon dioxide exchange: CarbonTracker, *Proceedings of the National Academy of Sciences* (*PNAS*) of the United States of America, 27 Nov. 2007, 104(48), 18925-18930, 2007.

Peylin, P., Law, R. M., Gurney, et al., Global atmospheric carbon budget: results from an ensemble of atmospheric CO_2 inversions, *Biogeosciences*, 10, 6699–6720, doi:10.5194/bg-10-6699-2013, URL http://www.biogeosciences.net/10/6699/2013/, 2013.

Pinty, B., G. Janssens-Maenhout, M. Dowell, H. Zunker, T. Brunhes, P. Ciais, D. Dee, H. Denier van der Gon, H. Dolman, M. Drinkwater, R. Engelen, M. Heimann, K. Holmlund, R. Husband, A. Kentarchos, Y. Meijer, P. Palmer and M. Scholze (2017) An operational anthropogenic CO_2 emissions monitoring & verification support capacity - Baseline requirements, Model components and functional architecture, doi:10.2760/39384, European Commission Joint Research Centre, EUR 28736 EN.

Poulter, B., Frank, D., Ciais, P., Myneni, R. B., Andela, N., Bi, J., Broquet, G. Canadell, J.G. Chevallier, F. Liu, Y. Y., Running, S. W., Sitch, S., and van der Werf, G. R.: Contribution of semi-arid ecosystems to interannual variability of the global carbon cycle. *Nature*, doi:10.1038/nature13376, 2014.

Prather, M.: Interactive comment on "Carbon dioxide and climate impulse response functions for the computation of greenhouse gas metrics: a multi-model analysis" by F. Joos et al, Atmos. Chem. Phys. Discuss., 12, C8465–C8470, www.atmos-chem-phys-discuss.net/12/C8465/2012/, 2012.

PSDv3, Product Specification Document (PSD) for the Essential Climate Variable (ECV) Greenhouse Gases (GHG) - Description of Common Parameters for core (ECA) products, Version 3, 6 June 2014. https://www.iup.uni-bremen.de/carbon_ghg/ghg-cci/PSDv3_GHG-CCI_final.pdf

Remaud, M., Chevallier, F., Cozic, A., Lin, X., and Bousquet, P.: On the impact of recent developments of the LMDz atmospheric general circulation model on the simulation of CO_2 transport, Geosci. Model Dev., 11, 4489–4513, https://doi.org/10.5194/gmd-11-4489-2018, 2018.

Reuter, M., Bovensmann, H., Buchwitz, M., et al., Retrieval of atmospheric CO_2 with enhanced accuracy and precision from SCIAMACHY: Validation with FTS measurements and comparison with model results, *J. Geophys. Res.*, 116, D04301, doi:10.1029/2010JD015047, 2011.

Reuter, M., Boesch, H., Bovensmann, H., et al., A joint effort to deliver satellite retrieved atmospheric CO_2 concentrations for surface flux inversions: the ensemble median algorithm EMMA, *Atmos. Chem. Phys.*, 13, 1771-1780, 2013.

Reuter, M., M. Buchwitz, M. Hilker, et al., Satellite-inferred European carbon sink larger than expected, *Atmos. Chem. Phys.*, 14, 13739-13753, doi:10.5194/acp-14-13739-2014, 2014a.

Reuter, M., M. Buchwitz, A. Hilboll, et al., Decreasing emissions of NOx relative to CO_2 in East Asia inferred from satellite observations, *Nature Geoscience*, 28 Sept. 2014, doi:10.1038/ngeo2257, pp.4, 2014b.

Reuter, M.: ESA Climate Change Initiative (CCI) Product User Guide version 4 (PUGv4) for the XCO2 SCIAMACHY Data Product BESD for the Essential Climate Variable (ECV): Greenhouse Gases (GHG), 31 August 2016, 2016a.

Reuter, M., M. Hilker, O. Schneising, M. Buchwitz, J. Heymann ESA Climate Change Initiative (CCI) Comprehensive Error Characterisation Report: BESD full-physics retrieval algorithm for XCO_2 for the Essential Climate Variable (ECV) Greenhouse Gases (GHG) Version 2.0, revision 1. 2016b.

Reuter, M., M. Buchwitz, M. Hilker, J. Heymann, H. Bovensmann, J. P. Burrows, S. Houweling, Y. Y. Liu, R. Nassar, F. Chevallier, et al., How much CO_2 is taken up by the European terrestrial biosphere?, Bulletin of the AmericanMeteorological Society, 0(0), doi:10.1175/BAMS-D-15-00310.1, 2016c.

Reuter, M., M. Buchwitz, O. Schneising, S. Noel, V. Rozanov, H. Bovensmann, J. P. Burrows, A Fast Atmospheric Trace Gas Retrieval for Hyperspectral Instruments Approximating Multiple Scattering - Part 1: Radiative Transfer and a Potential OCO-2 XCO_2 Retrieval Setup, Remote Sens., 9, 1159, doi:10.3390/rs9111159, 2017a.

Reuter, M., M. Buchwitz, O. Schneising, S. Noel, H. Bovensmann, J. P. Burrows, A Fast Atmospheric Trace Gas Retrieval for Hyperspectral Instruments Approximating Multiple Scattering - Part 2: Application to XCO_2 Retrievals from OCO-2, Remote Sens., 9, 1102, doi:10.3390/rs9111102, 2017b.

Reuter, M., Buchwitz, M., Schneising, O., Noël, S., Bovensmann, H., Burrows, J. P., Boesch, H., Di Noia, A., Anand, J., Parker, R. J., Somkuti, P., Wu, L., Hasekamp, O. P., Aben, I., Kuze, A., Suto, H., Shiomi, K., Yoshida, Y., Morino, I., Crisp, D., O'Dell, C. W., Notholt, J., Petri, C., Warneke, T., Velazco, V. A., Deutscher, N. M., Griffith, D. W. T., Kivi, R., Pollard, D. F., Hase, F., Sussmann, R., Té, Y. V., Strong, K., Roche, S., Sha, M. K., De Mazière, M., Feist, D. G., Iraci, L. T., Roehl, C. M., Retscher, C., and Schepers, D.: Ensemble-based satellite-derived carbon dioxide and methane column-averaged dry-air mole fraction data sets (2003–2018) for carbon and climate applications, Atmos. Meas. Tech., 13, 789–819, https://doi.org/10.5194/amt-13-789-2020, 2020.

Rödenbeck, C.: Estimating CO_2 sources and sinks from atmospheric mixing ratio measurements using a global inversion of atmospheric transport, Tech. Rep. 6, Max Planck Institute for Biogeochemistry, Jena, Germany, 2005.

Ross, A. N., Wooster, M. J., Boesch, H., Parker, R., First satellite measurements of carbon dioxide and methane emission ratios in wildfire plumes, *Geophys. Res. Lett.*, 40, 1-5, doi:10.1002/grl.50733, 2013.

Scarcle, J. D., Studies in astronomical time series analysis. III. Fourier transforms, autocorrelation functions and cross-correlation functions of unevenly spaced data. *Astrophys. J.*, 343, 874–887, 1989.

Schneising, O., Buchwitz, M., Reuter, M., et al., Long-term analysis of carbon dioxide and methane column-averaged mole fractions retrieved from SCIAMACHY, *Atmos. Chem. Phys.*, 11, 2881-2892, 2011.

Schneising, O., J. Heymann, M. Buchwitz, M. Reuter, H. Bovensmann, and J. P. Burrows, Anthropogenic carbon dioxide source areas observed from space: assessment of regional enhancements and trends, *Atmos. Chem. Phys.*, 13, 2445-2454, 2013.

Schneising, O., M. Reuter, M. Buchwitz, J. Heymann, H. Bovensmann, and J. P. Burrows, Terrestrial carbon sink observed from space: variation of growth rates and seasonal cycle amplitudes in response to interannual surface temperature variability, *Atmos. Chem. Phys*., 14, 133-141, 2014a.

Schneising, O., J. P. Burrows, R. R. Dickerson, M. Buchwitz, M. Reuter, H. Bovensmann, Remote sensing of fugitive methane emissions from oil and gas production in North American tight geologic formations, *Earth's Future*, 2, DOI: 10.1002/2014EF000265, pp. 11, 2014b.

Schulze, E. D., Luyssaert, S., Ciais, P., Freibauer, A., Janssens, I. A., Soussana, J. F., Smith, P., Grace, J., Levin, I., Tiruchittampalam, B., Heimann, M., Dolman, A. J., Valentini, R., Bousquet, P., Peylin, P., Peters, W., Rodenbeck, C., Etiope, G., Vuichard, N., Wattenbach, M., Nabuurs, G. J., Poussi, Z., Nieschulze, J., Gash, J. H., and Team, C.: Importance of methane and nitrous oxide emissions for europe's terrestrial greenhouse gas balance, *Nat. Geosci*., 2, 842–850, 2009.

Shindell, D. T., O. Pechony, A. Voulgarakis, et al., Interactive ozone and methane chemistry in GISS-E2 historical and future climate simulations, *Atmos. Chem. Phys.*, 13, 2653–2689, doi:10.5194/acp-13-2653-2013, 2013.

Somkuti, P.: ESA Climate Change Initiative (CCI) Product User Guide version 4.0 (PUGv4.0) for the University of Leicester full-physics XCO2 GOSAT data product (CO2_GOS_OCFP version 7) for the Essential Climate Variable (ECV): Greenhouse Gases (GHG), 31 August 2016, 2016.

Sussmann, R., Forster, F., Rettinger, M., and Bousquet, P.: Renewed methane increase for five years (2007–2011) observed by solar FTIR spectrometry, Atmos. Chem. Phys., 12, 4885-4891, doi:10.5194/acp-12-4885-2012, 2012.

Takahashi, T., Sutherland, S. C., Sweeney, C., Poisson, A., Metzl, N., Tilbrook, B., Bates, N., Wanninkhof, R., Feely, R. A., Sabine, C., Olafsson, J., and Nojiri, Y.: Global sea-air CO_2 flux based on climatological surface ocean pCO_2, and seasonal biological and temperature effects, *Deep Sea Res. II*, *49*, 1601–1623, 2002.

Takahashi, T., Sutherland, S. C., Wanninkhof, R., et al., Climatological mean and decadal changes in surface ocean pCO_2, and net sea-air CO_2 flux over the global oceans, *Deep-Sea Res. Pt. II*, 56, 554–577, doi:10.1016/j.dsr2.2008.12.009, 2009.

Turner, A. J., Jacob, D. J., Wecht, K. J., Maasakkers, J. D., Lundgren, E., Andrews, A. E., Biraud, S. C., Boesch, H., Bowman, K. W., Deutscher, N. M., Dubey, M. K., Griffith, D. W. T., Hase, F., Kuze, A., Notholt, J., Ohyama, H., Parker, R., Payne, V. H., Sussmann, R., Sweeney, C., Velazco, V. A., Warneke, T., Wennberg, P. O., and Wunch, D.: Estimating global and North American methane emissions with high spatial resolution using GOSAT satellite data, *Atmos. Chem. Phys*., 15, 7049-7069, doi:10.5194/acp-15-7049-2015, 2015.

Wanninkhof, R., Park, G. -H., Takahashi, T., Sweeney, C., Feely, R., Nojiri, Y., Gruber, N., Doney, S. C., McKinley, G. A., Lenton, A., Le Quéré, C., Heinze, C., Schwinger, J., Graven, H., and Khatiwala, S.: Global ocean carbon uptake: magnitude, variability and trends, *Biogeosciences*, 10, 1983-2000, doi:10.5194/bg-10-1983-2013, 2013.

van der Werf, G. R., Randerson, J. T., Giglio, L., Collatz, G. J., Mu, M., Kasibhatla, P. S., Morton, D. C., DeFries, R. S., Jin, Y., and van Leeuwen, T. T.: Global fire emissions and the contribution of deforestation, savanna, forest, agricultural, and peat fires (1997–2009), *Atmos. Chem. Phys*., 10, 11707-11735, doi:10.5194/acp-10-11707-2010, 2010.

Wecht, K. J., D. J. Jacob, C. Frankenberg, Z. Jiang, and D. R. Blake (2014), Mapping of North American methane emissions with high spatial resolution by inversion of SCIAMACHY satellite data, J. Geophys. Res. Atmos., 119, 7741–7756, doi:10.1002/2014JD021551.

Wunch, D., Toon, G. C., Blavier, J.-F., et al., The Total Carbon Column Observing Network, *Phil. Trans. R. Soc. A*, 369, 2087–2112, doi:10.1098/rsta.2010.0240, 2011.

Wunch, D. , Wennberg, P. O. , Toon, G. C. et al., A method for evaluating bias in global measurements of CO_2 total columns from space. Atmos. Chem. Phys., 11, 12317-12337, 2011.

York, D., Evensen, N., Martinez, M., and Delgado, J.: Unified equations for the slope, intercept, and standard errors of the best straight line. *Am. J. Phys*., 72(3), 367–375, 2004.

Yoshida, Y., Kikuchi, N., Morino, I., et al., Improvement of the retrieval algorithm for GOSAT SWIR XCO_2 and XCH_4 and their validation using TCCON data, *Atmos. Meas. Tech*., 6, 1533–1547, doi:10.5194/amt-6-1533-2013, 2013.

END OF DOCUMENT